Hindawi
Journal of Nanomaterials
Volume 2020, Article ID 1783749, 11 pages
https://doi.org/10.1155/2020/1783749

Research Article

Dual-Electronic Nanomaterial (Synthetic Clay) for Effective Removal of Toxic Cationic and Oxyanionic Metal Ions from Water

Van Phuong Nguyen,[1,2] Khanh Thien Tran Nguyen,[3] Loc That Ton,[4] Dong Thanh Nguyen,[5] Khuong Quoc Nguyen,[6] Mai Thi Vu,[7] and Hai Nguyen Tran[2,8]

[1]*Institute of Research and Development, Duy Tan University, Danang 550000, Vietnam*
[2]*Faculty of Environmental and Chemical Engineering, Duy Tan University, Da Nang City, Vietnam*
[3]*Department of Environment Sustainable Development, An Giang University, An Giang, VNU-HCM, Vietnam*
[4]*Department of Management Science, Thu Dau Mot University, Binh Duong, Vietnam*
[5]*Institute of Environmental Technology, Vietnam Academy of Science and Technology, Hanoi, Vietnam*
[6]*Department of Crop Science, College of Agriculture, Can Tho University, Can Tho, Vietnam*
[7]*Hanoi University of Natural Resources and Environment, Ministry of Natural Resources and Environment, Hanoi, Vietnam*
[8]*Institute of Fundamental and Applied Sciences, Duy Tan University, Ho Chi Minh City, Vietnam*

Correspondence should be addressed to Hai Nguyen Tran; trannguyenhai@duytan.edu.vn

Received 1 February 2020; Revised 30 March 2020; Accepted 21 May 2020; Published 7 September 2020

Academic Editor: Laura Martinez Maestro

A synthetic clay (Mg/Al-layered double hydroxides; LDH) was directly synthesized through a simple coprecipitation method under a low-supersaturation condition. The clay was applied to remove metal cations (Cd^{2+}, Cu^{2+}, Pb^{2+}, Ni^{2+}, and Cr^{3+}) and oxyanions (MnO_4^- and $Cr_2O_7^{2-}$) from a single aqueous solution. The result demonstrated that LDH exhibited a poor porosity (its specific surface area and total pore volume: 23.2 m^2/g and 0.161 cm^3/g, respectively) and positively charged surface within solution pH from 3.0 to 12. The X-ray powder diffraction (XRD) data suggested that the basal spacing of LDH was 0.773 nm. The presence of active CO_3^{2-} anions in the interlayer region of LDH that played an extremely important role in the adsorption process was identified by XRD and Fourier-transform infrared spectroscopy (FTIR). Energy-dispersive X-ray spectroscopy (SEM) analysis indicated that LDH possessed a surface morphology like a plate with a hexagonal shape. The adsorption isotherms of LDH towards various potentially toxic metals were conducted at 1.0 g/L, $pH_{Equilibrium}$ 5.0, 30°C, and 24 h. The Langmuir maximum adsorption capacity of LDH towards the target metals exhibited the following order: 1.299 mmol/g (for Ni^{2+} adsorption) > 0.880 mmol/g (Cd^{2+}) > 0.701 mmol/g (Cr^{3+}) > 0.657 mmol/g (Pb^{2+}) > 0.601 mmol/g (Cu^{2+}) > 0.589 mmol/g ($Cr_2O_7^{2-}$) > 0.522 mmol/g (MnO_4^-). The synthetic clay can adsorb both cations and anions in the solution. Therefore, such LDH material can serve as a potential dual-electronic adsorbent for effectively eliminating various oxyanionic and cationic metal ions from water media.

1. Introduction

The appearance of potentially toxic metals in water bodies has caused more enormous concerns such as potential health risks for humans and environmental threats because of their high toxicity. In real wastewater, anionic and cationic contaminants always coexist in such environment. Therefore, it is necessary to explore and develop some advanced adsorbents with their excellent adsorption capacity towards various kinds of toxic contaminants, although commercial activated carbon (CAC) with its extremely high porosity has been acknowledged as a potential adsorbent for removing various contaminants from a water environment through pore-filling adsorption mechanism [1]. However, CAC, which is a high energy-consuming material, is expensive (~3 USD/kg) because it is often prepared through

a pyrolysis process at high temperatures (>800°C) along with certain activation (i.e., physical or chemical) [2, 3]. Furthermore, an adsorption process related to pore-filling mechanism is usually irreversible for the adsorption of organic contaminants with a large molecule size (i.e., dye). Therefore, contaminant-laden AC cannot be effectively used for regeneration [2]. For example, Tran et al. [3] investigated the adsorption process of cation methylene green dye onto three kinds of AC material. They found that desorption efficiency was negligible when a chemical desorption method was used. In addition, Tomul et al. [4] concluded that the desorption of naproxen from three laden biochar samples by a chemical method was less efficient than that by a thermal method. However, the mass loss during the thermal method should be considered, such as approximately $13\% \pm 2.5$, $17\% \pm 7.4$, $34\% \pm 8.4$, and $41\% \pm 0.95$ for each cycle of adsorption/desorption.

In general, layered double hydroxides (LDH) are normally known as hydrotalcite-like minerals/solids or synthetic anionic clays. The structure of LDH is composed of two oppositely charged parts: (1) the positively charged brucite-like sheets and (2) negatively charged anionic interlayers [5, 6]. The general formula of LDH is often expressed as $[M^{2+}_{1-x}M^{3+}_{x}(OH)_2]^{x+}(A^{n-})_{x/n} \cdot mH_2O$ [6]. In this formula, M^{2+} represents the divalent metal cations (i.e., Mg^{2+}), M^{3+} the trivalent metal cations (i.e., Al^{3+}), A^{n-} the interlayer charge-balancing anions of valence n (i.e., CO_3^{2-}), and x the $M^{3+}/(M^{2+} + M^{3+})$ molar ratio (ranging from 0.20 to 0.33) [6, 7]. According to the literature, LDH has been successfully synthesized by numerous methods (i.e., coprecipitation, ion exchange, hydrothermal method, and rehydration using a structural memory effect) [8]. Of those methods, coprecipitation prepared at a low supersaturation has been considered the most appropriate method for synthesizing LDH because of its simplicity in generating LDH with a high crystalline structure [6, 9]. The resultant LDH precipitates can be classified as a typical nanomaterial, with their size distribution being approximately 270 nm for Ni/Fe-LDH [10], 370 nm for Zn/Al-LDH [11], and 469 nm for glycerol-modified Ni/Fe-LDH [10].

The structural and morphological characteristics of LDH are strongly dependent on the synthesis process and the nature of used metal salts [10–12]. For example, LDH is synthesized from metal salts of nitrate (i.e., $Al(NO_3)_3$); the interlayer region of LDH often contains the NO_3^{2-} anions [6]. In addition, during the coprecipitation process of metal salts, CO_3^{2-} anions can be performed in the interlayer region of LDH because CO_2 gas is commonly dissolved in water. The presence of CO_3^{2-} anions in such region can be minimized if nitrogen gas flow is sufficiently used during coprecipitation to prevent the existence of CO_3^{2-} anions in solution. However, some previous studies demonstrated that the presence of host anions (i.e., CO_3^{2-}) in the interlayer region can serve as active exchangeable sites for removing various contaminant anions from water. Such anions comprise (1) inorganic contaminants: hexavalent chromium anion (i.e., CrO_4^{2-} and $Cr_2O_7^{2-}$) [10, 12–14], arsenate anion ($H_2AsO_4^-$ and $HAsO_4^{2-}$) [12, 15, 16], and antimonate anion ($Sb(OH)_6^-$) [15] as well as (2) organic contaminants: anionic reactive blue 21 dye [17], anionic methyl orange dye [18], three other anionic dyes (i.e., Congo red, indigo carmine, and sunset yellow FCF) [19], and anticancerous drug methotrexate [11]. Furthermore, the important role of CO_3^{2-} anions in the interlayer region in effectively removing potentially toxic metals from water through precipitation mechanism (i.e. $CdCO_3$) has been acknowledged in the literature. Such cationic metals include Cu^{2+} [9, 20–22], Zn^{2+} [20, 22, 23], Pb^{2+} [14, 22–24], Cd^{2+} [9, 23], Ni^{2+} [9], and Eu^{3+} [21]. To sum up, LDH can be classified as a "*dual-electronic adsorbent*" because of its unique structure characterization: positively charged sites on its external surface (high positively ζ potential value) and abundantly exchangeable anions within its interlayer region (high anion exchange capacity).

Recently, some authors developed LDH modified with anionic surfactant sodium dodecyl sulfate (SDS) [18]. The resultant hierarchical flower-like LDH exhibited a hydrophobic surface with a high-water contact angle of 90.1°. Such LDH solid can be classified as an "*amphiphilic adsorbent*" to remove both polar and nonpolar organic compounds (i.e., anionic methyl orange dye and naphthalene) through adsorption and partition processes, respectively. However, the term of amphiphilic adsorbent is only for LDH modified with a certain anionic surfactant, not for pristine LDH (without any additional modification or treatment).

Furthermore, previous research indicated that Ca/Al-LDH can effectively remove chemical oxygen demand (COD; 73.9%), UV254 (85.8%), and total organic carbon (TOC; 74.7%) from water [25]. The authors [25] also found that COD removal by the LDH material (73.9%) was higher than that by the ion exchange resin (only 60%). Notably, Rahman and colleagues [22] compared sludge volume formed during the removal process of heavy metals using Mg/Al-LDH and $Ca(OH)_2$. They found that using Mg/Al-LDH for removing heavy metals only produced almost half as much sludge as using $Ca(OH)_2$. A similar trend of sludge reduction was obtained when comparing the application of Mg/Al-LDH and $Ca(OH)_2$ in treating the acidic mine wastewater [16]. Therefore, application of LDH for water treatment can minimize the major problems regarding sludge disposal.

In essence, each adsorbent material often exhibits an excellent affinity to each type of pollutant (i.e., cationic or anionic adsorbate). To tackle such problem, a dual-electronic material is developed by applying several further processes (i.e., modification, treatment, or grafting). After those processes, the dual-electronic material can simultaneously remove both cationic and anionic pollutants from the water environment. For example, Chao and Chen [26] prepared hexadecyltrimethylammonium bromide-(HDTMA-) modified NaY zeolite, concluding that this dual-electronic material can well adsorb both cationic (Cu^{2+}, Zn^{2+}, Ni^{2+}, Pb^{2+}, and Cd^{2+}) and oxyanionic metal ($Cr_2O_7^{2-}$ and MnO_4^-) ions in solution. An analogous conclusion was found for other materials—titanate nanotubes modified with hexadecyltrimethylammonium [27] and mesoporous silicas functionalized with amine and nitrilotriacetic acid anhydride [28].

Layered double hydroxides without further modification or treatment process are highly expected to remove both cationic and oxyanionic metal ions from solution through their

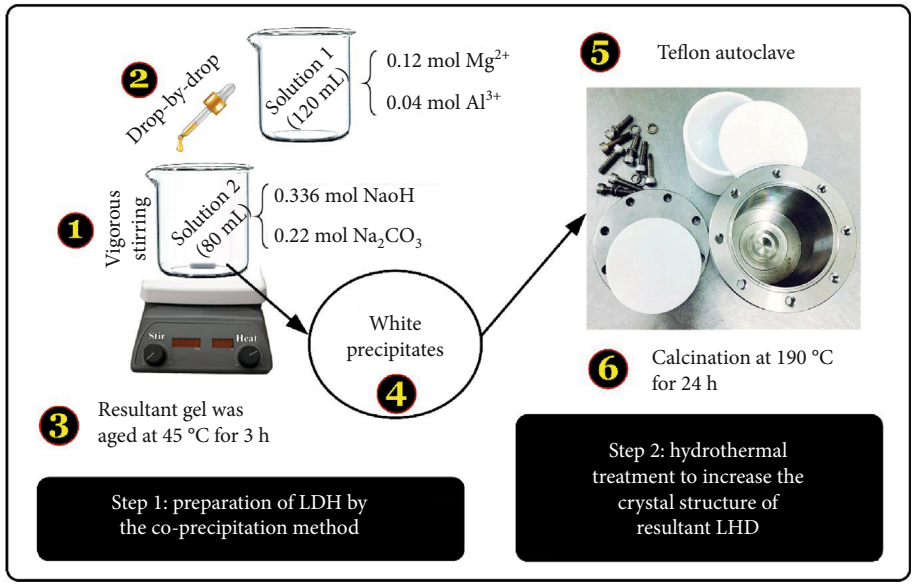

Figure 1: Producer for preparation of Mg/Al-layered double hydroxides by the coprecipitation process.

unique properties. Therefore, in this study, a dual-electronic nanomaterial derived from layered double hydroxides was directly synthesized by a simple coprecipitation method. A hydrothermal treatment was subsequently used to further improve the crystalline structure of LDH. The synthesized nanomaterial was characterized by textual property, surface morphology and functionality, zeta potential, and crystalline structure. It was then applied as a potential adsorbent to adsorb five cationic metals (Cd^{2+}, Cu^{2+}, Pb^{2+}, Ni^{2+}, and Cr^{3+}) and two oxyanion metals (MnO_4^- and $Cr_2O_7^{2-}$) in single aqueous solution. The relevant adsorption mechanism was also discussed herein.

2. Material and Method

2.1. Chemicals. Whole chemicals used in this investigation were of analytical reagent grade, so they were directly used without any further purification. Aluminum nitrate 9-hydrate and magnesium nitrate hexahydrate were bought from Merck. Sodium carbonate and sodium hydroxide puriss were purchased from BAKER. Four selective divalent cation metals include cadmium nitrate tetrahydrate (purchased from Alfa Aesar), nickel(II) nitrate hexahydrate (Merch), copper(II) nitrate trihydrate (Merch), and lead(II) nitrate (Sigma-Aldrich). One trivalent cation metal (chromium(III) nitrate nonahydrate) was delivered from Merch. Meanwhile, two oxyanionic metal ions—potassium permanganate and potassium dichromate—were selected from Sigma-Aldrich and Merch, respectively. Deionized distilled high-purity water was obtained from a Milli-Q water (Millipore) system.

2.2. Preparation of Layered Double Hydroxides. The Mg/Al-LDH nanoparticles were synthesized through a two-step process: coprecipitation and thermal crystallization [29]. Briefly, the mixture solution of $Mg(NO_3)_2{\cdot}6H_2O$ and $Al(NO_3)_3{\cdot}9H_2O$ was added dropwise into another (NaOH and Na_2CO_3) under stirring. The pH of the solution was controlled at approximately 12 ± 0.3 for 3 h at 45°C to obtain white precipitates. Notably, nitrogen gas was not used during the precipitation process to expect the spontaneous formation of abundant CO_3^{2-} anions in the interlayer region of LDH. Subsequently, the solution containing the precipitates was transferred into a Teflon-lined autoclave. The autoclave was then heated at 190°C for 24 h (Figure 1). The resultant nanoparticles were collected by centrifugation, washed repeatedly with pure water, dried at 60°C for 48 h, and stored in a desiccator until further use. A primary test was conducted to explore the effect of Mg/Al molar ratios (i.e., 1 : 1, 2 : 1, 3 : 1, 4 : 1, and 5 : 1) on the adsorption capacity of LDH to the selective metals. The adsorption results in Figure 2 indicated that an increase in the Mg/Al ratio from 1 : 1 to 3 : 1 resulted in increasing the adsorption capacity of LDH to Ni^{2+} and $Cr_2O_7^{2-}$ ions in a single solution. However, a further increase in the ratio to 5 : 1 caused a significant decrease in the adsorption capacity of the LDH towards Ni(II) cation or an insignificant change of the adsorption capacity of the LDH towards Cr(VI) anion. Therefore, the molar ratio of M^{2+} to M^{3+} of 3 : 1 was selected for further studies of the characterization of LDH and the adsorption of potentially toxic metals in solution.

2.3. Characterization of Layered Double Hydroxides. X-ray diffraction (XRD) data were obtained from a PANalytical PW3040/60 X'Pert Pro. Fourier-transform infrared (FT-IR) spectrum was detected by a PerkinElmer 1600 FT-IR spectrophotometer. A scanning electron microscope (SEM, S-3000N, Hitachi) was used to measure the morphological surface property of LDH. The external surface charge of LDH was analyzed by a zeta potential analyzer (Colloidal Dynamics; ZED-3600). The porosity of LDH was calculated from the nitrogen adsorption/desorption isotherm (Micromeritics ASAP 2020 sorptometer) at 77 K. The LDH sample had been

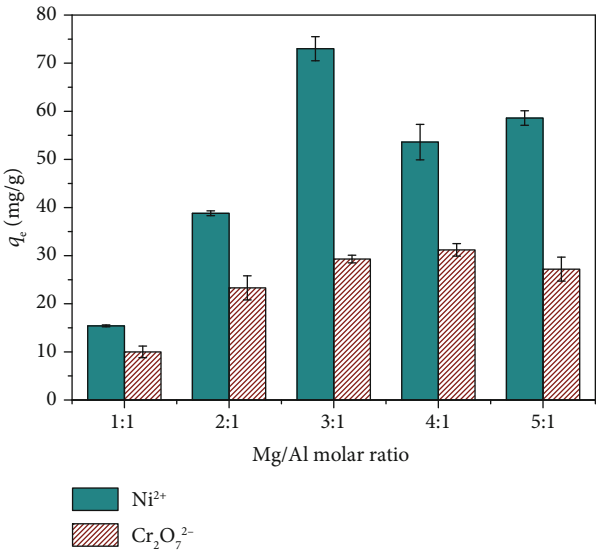

Figure 2: Effect of the Mg/Al molar ratio on the adsorption capacity of LDH (experimental conditions: C_o =188 mg/g for Ni and 191 mg/L for Cr(VI), pH = 5.0, 24 h, and 30°C).

dried in a vacuum oven at 105°C for 24 h before it was used for analyzing its aforementioned properties.

2.4. Study of Adsorption Isotherm. The study of adsorption isotherm was concluded in a single metal solution to avoid the phenomenon of competitive adsorption. Adsorption conditions were described as follows: a solid/liquid ratio of 1.0 g/L (m/V), temperature of 30°C, contact time of 48 h, and controlled solution pH of 5.0. The concentration of toxic metal ions before and after adsorption was determined by an Inductively coupled plasma mass spectrometry (ICPMS-NexION 2000, US). The blank sample (the initial concentration of adsorbate without the presence of LDH denoted as the C_o value) was conducted simultaneously. The amount of metal adsorbed by LDH (q_e; mmol/g) was calculated from the mass balance equation (Equation (1)). Each study of adsorption was conducted in triplicate, and the average values were reported.

In this study, the Langmuir model (Equation (2)) [30] was applied to estimate the maximum adsorption capacity of LDH towards each target metal. Meanwhile, the Freundlich model [31] (Equation (3)) is commonly used for the real design of water system because it is an empirical equation. Two adsorption isotherm models have been widely applied in the literature to model the experimental data of adsorption equilibrium because of the help of their parameters [3, 5, 7, 32, 33]. The important role of the parameters of two selective models in the adsorption process was discussed in Section 3.2.

$$q_e = \frac{(C_o - C_e)}{m} V, \tag{1}$$

$$q_e = \frac{(Q^o_{max} K_L C_e)}{1 + K_L C_e}, \tag{2}$$

$$q_e = (K_F \times C_e^n), \tag{3}$$

where C_o and C_e (mmol/L) are the concentrations of metal in solution before and after equilibrium adsorption, respectively; m (g) is the mass of used LDH; V (L) is the volume of the metal solution; Q^o_{max} (mmol/g) is the maximum saturated adsorption capacity of LDH; K_L (L/mmol) is the Langmuir constant related to the affinity between metal and LDH; K_F [(mmol/g)/(L/mmol)^n] is the Freundlich constant, which characterizes the strength of adsorption; and n (dimensionless; $0 < n < 1$) is a Freundlich intensity parameter, which indicates the magnitude of the adsorption driving force or surface heterogeneity; the adsorption isotherm becomes linear with $n = 1$, favorable with $n < 1$, and unfavorable with $n > 1$.

To minimize error functions during modeling, a nonlinear optimization technique was applied for computing the relevant parameters of the selective models [32]. The adjusted coefficient of determination (Adj-R^2) and chi-square test (χ^2) were automatically calculated from the Origin software; meanwhile, standard deviation of residues (SD), Marquardt's percent standard deviation (MPSD) [34], and Bayesian information criterion (BIC) [35] are expressed in Equation (4), (5), and (6), respectively. The best fitting model exhibits the highest Adj-R^2 value, but the lowest value of the others (i.e., χ^2, SD, MPSD, and BIC).

$$\mathrm{SD} = \sqrt{\left(\frac{1}{n-p}\right)\left[\sum\left(q_{e,exp} - q_{e,model}\right)^2\right]}, \tag{4}$$

$$\mathrm{MPSD} = 100\sqrt{\left(\frac{1}{n-p}\right)\left[\sum\left(\frac{q_{e,exp} - q_{e,model}}{q_{e,exp}}\right)^2\right]}, \tag{5}$$

$$\mathrm{BIC} = n \ln\left[\frac{\sum\left(q_{e,exp} - q_{e,model}\right)^2}{n}\right] + [p \ln(n)], \tag{6}$$

where $q_{e,exp}$ is the amount of adsorbate in solution adsorbed by adsorbent from the experiment (calculated from Equation (1)); $q_{e,model}$ is the amount of adsorbate in solution adsorbed by adsorbent estimated from the selective model; n is the number of experimental points used for modelling; and p is the number of parameters in the selective model.

3. Results and Discussion

3.1. Property of Layered Double Hydroxides. The structure feature of LDH was confirmed by the XRD spectrum (Figure 3). As expected, the synthesized LDH was a typically well-crystallized material. Two shaped diffraction peaks observed at two-theta degree of 11.44° (a typical 003 characteristic) and 22.82° (006) were consistent with the standard JCPDS file of the hydrotalcite structure (JCPDS No. 89–0460) and in the literature [12, 36]. According to the Bragg's law, the basal spacing (d_{003}) of LDH was calculated to be 0.773 nm. An identical result was reported for similar

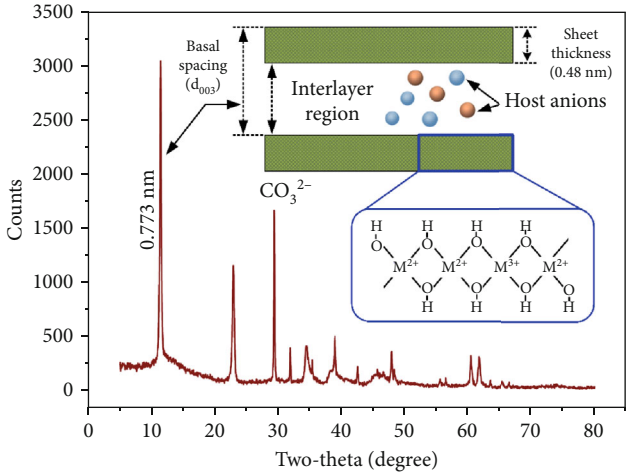

Figure 3: X-ray powder diffraction of the layered double hydroxides.

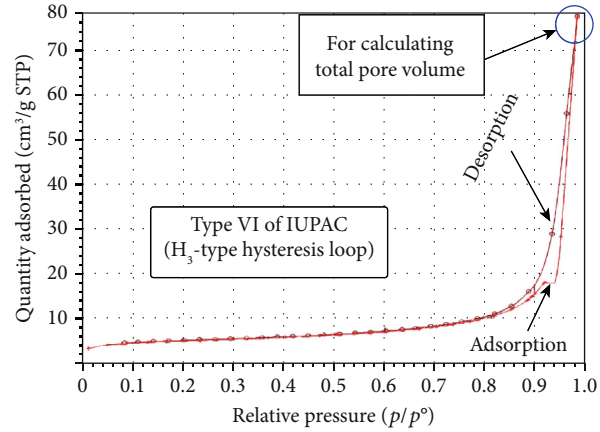

Figure 4: Nitrogen gas adsorption/desorption isotherm onto LDH at 77 K.

Table 1: Textural parameters of the prepared LDH nanoparticles.

	Unit	Value
(1) Surface area		
Langmuir surface area	m^2/g	119
BET surface area	m^2/g	23.2
External surface area	m^2/g	15.2
Micropore surface area	m^2/g	8.05
(2) Pore volume		
Total pore volume	cm^3/g	0.161
Mesopore volume	cm^3/g	0.157
Micropore volume	cm^3/g	0.004
(3) Pore width		
Average pore width	nm	27.8

Mg/Al-LDH materials (i.e., 0.80 nm [22], 0.780 nm [15], 0.769 nm [19], 0.762 nm [37], 0.760 nm [14], and 0.758 nm [12]) and for the other LDH (Zn/Al-LDH (0.887 nm) [11], Ni/Fe-LDH (0.782 nm) [10], Mn/Mg/Fe-LDH (0.777 nm) [24], and Zn/Al-LDH (0.755 nm) [17]). In addition, because the host CO_3^{2-} anions were abundantly presented in the interlayer region of LDH (confirming by the XRD spectrum at 29.39°), the synthesized nanoparticles can be classified as LDH containing the interlayer carbonate anions (CO_3-LDH). The carbonate anions can (1) effectively interact with selective cationic metals (i.e., cadmium) in solution to form the metal-carbonate precipitation [5] or (2) provide the exchangeable anion sites towards oxyanionic metals (i.e., dichromate) in solution [6, 7].

The isotherm of nitrogen gas adsorption/desorption onto LDH is illustrated in Figure 4. According to the report of physisorption data for gas/solid systems published by IUPAC [38], the physisorption exhibited a typical characteristic feature of Type IV isotherm, with a type H3 hysteresis loop being observed at a relative pressure (p/p_o) higher than 0.8 [19]. The IV-type isotherm combined with H3-type loop was an indication of mesoporosity with slit-shaped pores [6, 10, 18]. An analogous observation has been reported elsewhere [12, 36]. Furthermore, the textural property of LDH (Table 1) obtained from the physisorption isotherm indicated that LDH was a nonporous material. This is because it exhibited a low Brunauer-Emmett-Teller (BET) surface area ($S_{BET} = 23.2\ m^2/g$) and total pore volume ($V_{Total} = 0.161\ cm^3$). Similarly, some scholars reported that LDH solids exhibited a low specific surface area and total pore volume, such as Mg/Al-LDH ($S_{BET} = 51.0\ m^2/g$ and $V_{Total} = 0.236\ cm^3/g$) [19], Ni/Fe-LDH ($34.2\ m^2/g$ and $0.06\ cm^3/g$) [10], Mg/Al-LDH ($15.7\ m^2/g$ and $0.078\ cm^3/g$) [37], and hierarchical flower-like Mg/Al-LDH ($3.58\ m^2/g$ and $0.076\ cm^3/g$) [18]. This means that the adsorption of selective metals through well-known pore-filing mechanism seems negligible [6]. In this case, LDH can remove potentially toxic metals from water media through other adsorption mechanisms (e.g., surface precipitation, complexation, and ion exchange).

The main functional groups on the LDH's surface were qualitatively detected by FTIR (Figure 5). Several corresponding key bands were highlighted and provided in the FTIR spectrum. Firstly, a broad band at approximately $3500\ cm^{-1}$ is designated to the –OH group of the hydroxide layers, interlayer water molecules, and even moisture. Secondly, a profound band at nearly $1640\ cm^{-1}$ is assigned to the C=O overlapped N=O functional groups in the interlayer region that might mainly correspond to the interlayer CO_3^{2-} and NO_3^- anions, respectively. Thirdly, the overlapping of C–O (relative to host CO_3^{2-} anion) and N–O (host NO_3^- anion) vibration is well-identified at around $1370\ cm^{-1}$. Lastly, two bands corresponding to the metals (M=Mg and Al) vibrations are observed at approximately $676\ cm^{-1}$ (O–M–O) and $420\ cm^{-1}$ (M–OH) [6, 12, 36, 37, 39]. The result suggested that (1) LDH might contain the abundant host anions (CO_3^{2-} and NO_3^-) in the interlayer region and (2) the external surface of LDH might be positively charged because of the abundant presence of –OH groups (primarily derived from Al–OH and Mg–OH) on its surface.

In essence, the pKa value of the hydroxyl group is often higher than 11 [40]. Therefore, the –OH group is protonated into the $-OH_2^+$ group when solution pH < its pKa value. This is well consistent with the analysis result of zeta potential of

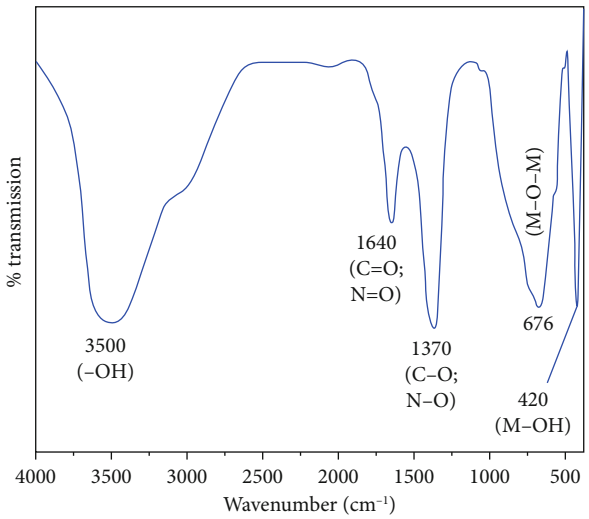

Figure 5: FTIR spectrum of the layered double hydroxides.

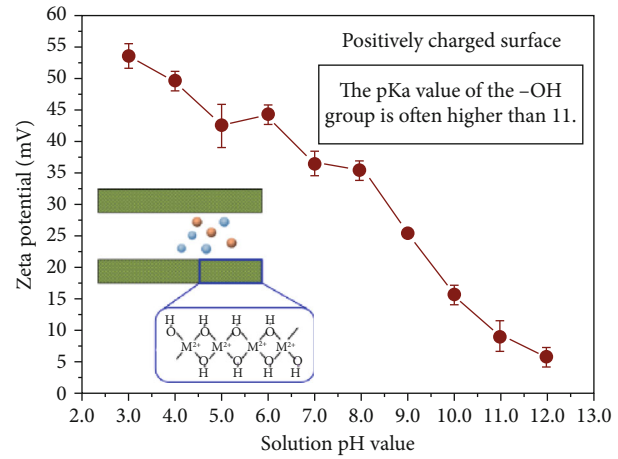

Figure 6: Zeta potential of the layered double hydroxides under different solution pH.

LDH (Figure 6). The zeta (ζ) potential values of LDH were positive, suggesting that the external surface of LDH was highly positively charged within the solution pH range from 3.0 to 12. Similarly, Lee and coworkers [15] reported that the pH values of isoelectric point (IEP) of Mg/Al-LDH, LDH calcinated at 400°C, and LDH calcinated at 600°C were 12.1 (pH_{IEP}), 12.7, and 12.5, respectively. An identical observation was summarized in a recent review article [6]. Furthermore, LDH had a high positive ζ value at pH 5.0 (42.5 ± 3.5 mV) and 6.0 (44.2 ± 1.5 mV) which is consistent with the report of Abo El-Reesh and coworkers [10] for Ni/Fe-LDH (43.3 mV at pH 6.0) and glycerol-modified Ni/Fe-LDH (32.8 mV at pH 6). The result suggested that LDH exhibited a high affinity to anions in solution through electrostatic attraction.

Finally, as portrayed by SEM image (Figure 7), LDH exhibited a plate-like morphology on the surface. This is a typical morphology of synthesized LDH materials. As aforementioned in Section 1, the morphology of LDH strongly depended on the synthesis process and the nature of used metal salts. Different morphologies of LDH were observed in the literature such as the morphology like sheet [22], nanofoil [11], 3D hierarchically flower [12, 18], and interconnecting flower [20]. To some extent, the morphological property of LDH has a less impact on its adsorption capacity compared to the others (i.e., its surface area and charge).

3.2. Adsorption Isotherm. The adsorption isotherms of target potentially toxic metals onto LDH are presented in Figure 8. The pH solutions were maintained at around 5.0 ± 0.2 to avoid the precipitation in the form of metal hydroxide (also known as precipitation by pH). For example, copper metal ions can be spontaneously precipitated in solution in the form of $Cu(OH)_2$ without being adsorbed by LDH when solution pH values are higher than 6.0. Furthermore, in a low solution pH value (i.e., 2.0), the structure of the synthesis clay might not be stable. This is because the LDH particles were synthesized through the coprecipitation process at a high pH value of 12 (Section 2.1). In other words, the synthesized particles had a low chemical stability under acidic solution.

According to the shape classification of adsorption isotherm [41], the shape of the adsorption isotherms of metal cations and oxyanions was categorized as L-type or F-type (not H-type) without a strict plateau. The relationship between isotherm parameters and isotherm shapes has been analyzed by Tran and coworkers [32]. The value of the n parameter of the Freundlich model in Table 2 ranged from 0.203 to 0.446 (lower 1.0), suggesting that the adsorption isotherm was favorable. The conclusion was confirmed by the concave downward curve of adsorption isotherm in Figure 8. The outcome suggested that LDH tended to exhibit a higher affinity to the pollutants under high concentrations in solution. Therefore, it should be given a considerable concern when LDH is applied to remove the pollutants under their low concentrations (or trace levels) from the water environment.

The corresponding parameters of the Langmuir and Freundlich models (Table 2) were calculated from the nonlinear optimization method to minimize the error function during modeling. According to a higher adjusted coefficient of determination, the Langmuir model (Adj-$R^2 = 0.985$–0.994) was more appropriate to describe the experimental data of equilibrium adsorption of the target metals by LDH than the Freundlich model (Adj-$R^2 = 0.853$–0.962) did. This conclusion is well consistent with the result of other statistics; for example, the value of χ^2, SD, MPSD, and BIC of the Langmuir model was lower than that of the Freundlich model (Table 2). As expected, the prepared LDH can effectively adsorb cationic and oxyanionic metal ions in aqueous solutions. This means that it can serve as a promising dual-electronic adsorbent for removing both cationic and anionic pollutants from water media.

In general, the Freundlich model can be applied for estimating the maximum adsorption capacity of an adsorbent when adsorption shape is nearly linear (the n parameter ≈ 1.0). The linear isotherm shape is commonly known as the partition phenomenon [26]. In this study, the n parameter was lower than 1.0; therefore, the

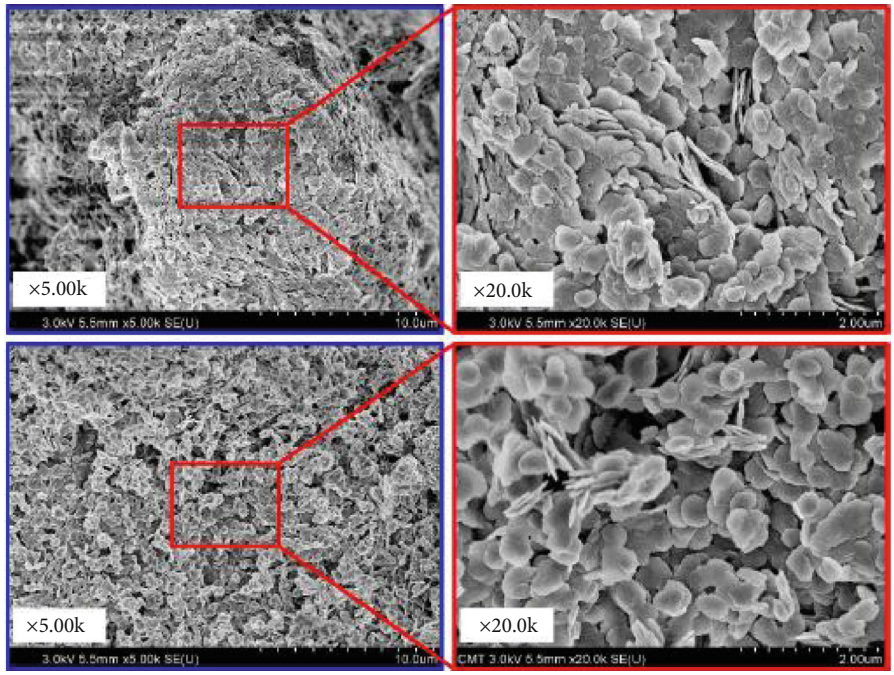

Figure 7: SEM image of the layered double hydroxides at different magnifications.

maximum adsorption capacity of LDH was estimated through the Langmuir model. Under the same operational conditions of adsorption study, the maximum adsorption capacity (Q^{o}_{max}) of LDH towards the potentially toxic metals exhibited the following order: 1.299 mmol/g (for Ni^{2+} adsorption) > 0.880 mmol/g (Cd^{2+}) > 0.701 mmol/g (Cr^{3+}) > 0.657 mmol/g (Pb^{2+}) > 0.601 mmol/g (Cu^{2+}) > 0.589 mmol/g ($Cr_2O_7^{2-}$) > 0.522 mmol/g (MnO_4^{-}). The result suggested that CO_3-LDH possessed a higher adsorption capacity of cationic metals than anionic ones in solution. This is because the precipitation mechanism between cationic metal ion in solution and CO_3^{2-} anion in the interlayer region of LDH (i.e., $CdCO_3$) was more dominant than anion exchange mechanism between anionic metal ion in solution and CO_3^{2-} anion in LDH. In addition, the cationic metal ions highly tended to react with the –OH groups on the external surface of LDH through nonelectrostatic attraction (inner-sphere complexation).

Because most LDH materials have applied for the removal of hexavalent chromium from water, such adsorbate was selected as a target pollutant for comparison. The Mg/Al-LDH adsorbent (Q^{o}_{max} = 127.3 mg/g) exhibited a higher adsorption capacity towards Cr(VI) that the other LDH materials reported in the literature, such as Mg/Al-LDH (16.3 mg/g) [42], Ni/Fe LDH (50.4 mg/g) [10], Mg/Al-LDH (58.8 mg/g) [37], and Mg/Al-LDH calcinated at 500°C (65.2 mg/g) [12]. Notably, a higher zeta potential value of Mg/Al-LDH (42.7 mV) in this study compared to that of Mg/Al-LDH (~18 mV) reported by other researchers [37] might lead to a higher affinity to Cr(VI) in solution through electrostatic attraction. As a result, the prepared Mg/Al-LDH adsorbent (127.3 mg/g) exhibited a remarkably higher maximum adsorption capacity than the Mg/Al-LDH one (58.8 mg/g) reported by Zhu and colleagues [37]. Interestingly, the synthesized Mg/Al-LDH nanomaterial (Q^{o}_{max} = 127.3 mg/g) possesses an outstanding adsorption capacity compared to activated carbon (103 mg/g) and biochar (83.5 mg/g) [43], HDTMA-modified zeolite (39.7 mg/g) [26], and HDTMA-modified titanate nanotubes (18.6 mg/g) [27].

3.3. Feasible Adsorption Mechanism. In essence, the mechanism of pollutant adsorption is often strongly dependent on the solution pH value. This is because solution pH greatly affects both the species of adsorbate and the surface of adsorbent. In this study, potential adsorption mechanisms were discussed at the solution of $pH_{Equilibrium}$ 5.0.

As shown in Figure 6, the prepared LDH adsorbent exhibited a positively charged surface because of its positive ζ value of 42.7 mV. Therefore, electrostatic attraction was ruled out for the adsorption of cationic metal ions, but the integral contribution to the adsorption of oxyanionic metal ions onto LDH. Furthermore, a previous study indicated that the abundant presence of CO_3^{2-} anions in the interlayer region of LDH can spontaneously simulate the precipitation process occurring between cationic metals (i.e., Pb^{2+} and Cu^{2+}) and carbonate ions to form carbonate hydroxides (i.e., $Pb_3(OH)_2(CO_3)_2$ and $Cu_2CO_3(OH)_2$, respectively) [9, 24]. In addition, Rahman and coworkers [22] analyzed the precipitates (characterized by XRD) after the adsorption process of heavy metals (Cu^{2+}, Pb^{2+}, and Zn^{2+}) onto LDH. They found the important role of host NO_3^{2-} anions in the interlayer region of Mg/Al-LDH in removing potentially toxic metals. The formed precipitates after the adsorption process included copper nitrate hydroxide [$Cu_2(OH)_3NO_3$], lead nitrate hydroxide [$Pb_4(OH)_4(NO_3)_4$], zinc nitrate hydroxide hydrate [$Zn(NO_3)(OH)H_2O$], and zinc nitrate hydroxide [$Zn_5(NO_3)_2(OH)_8$]. In this study, the interlayer region of Mg/Al-LDH contained both the host CO_3^{2-} and NO_3^{-} anions. Therefore, it is expected that the precipitates in the

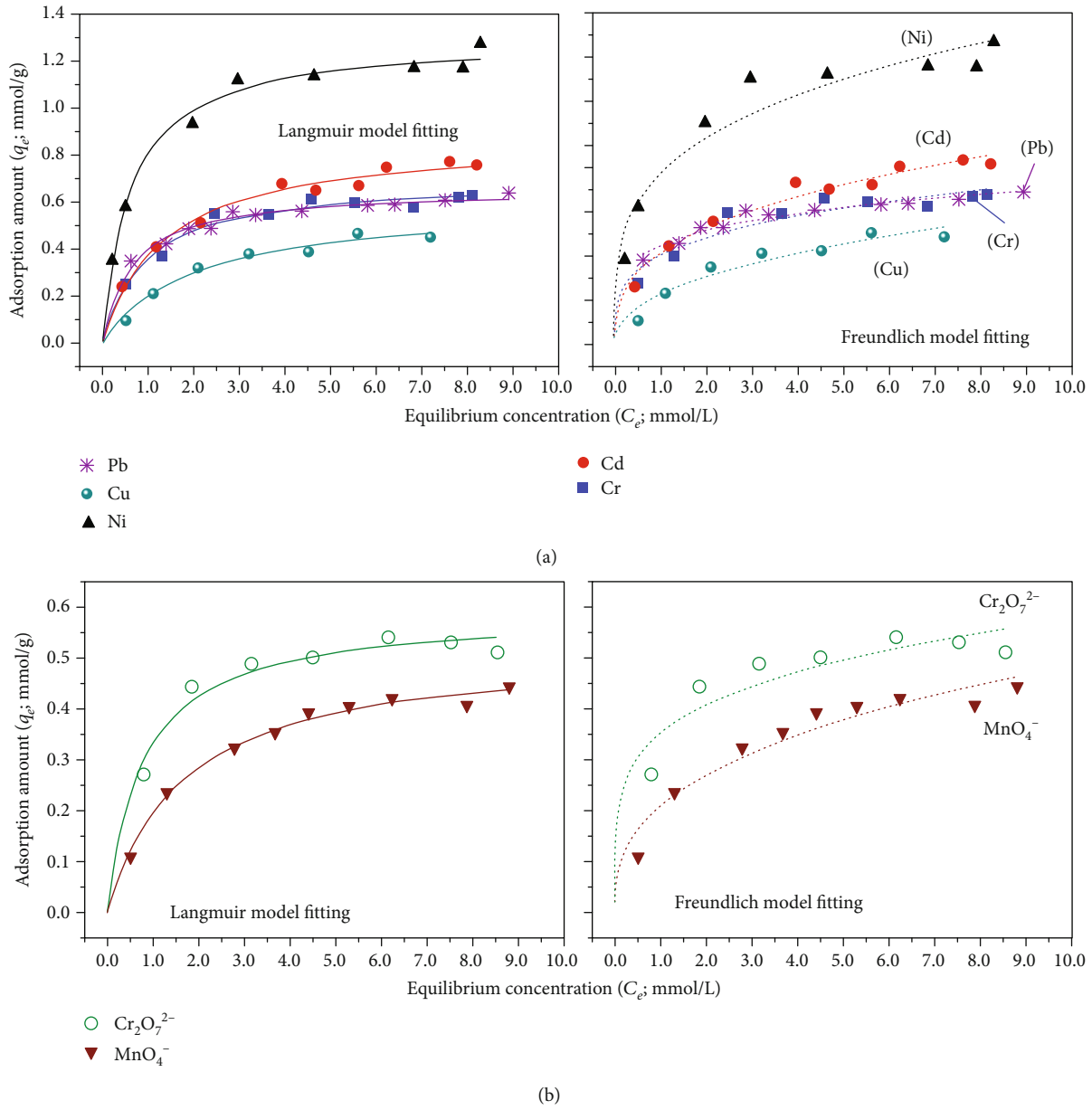

Figure 8: Adsorption isotherm of (a) cationic metal ions and (b) oxyanionic metal ions onto the prepared LDH nanoparticles.

form of carbonate and nitrate were formed after the adsorption process. This mechanism might be dominant than the others (i.e., isomorphic substitution and complexation).

Notably, LDH abundantly contained the –OH group on its surface; such group can act as an active site to binding cationic metal ions in solution through surface complexation [5]. For example, Zhao and coworkers [20] applied the X-ray photoelectron spectroscopy (XPS) spectrum of Cu 2p and Zn 2p and concluded that the surface complexation occurred between the OH groups on the external surface of Li/Al-LDH and Cu^{2+} or Zn^{2+} ions. An identical conclusion was obtained for the adsorption of Pb^{2+} ions onto Mn/Mg/Fe-LDH [24], Cu^{2+} ions onto sulfonated calix[4]arene intercalated Mg/Al-LDH [21], and Pb^{2+}, Cu^{2+}, Cd^{2+}, and Zn^{2+} onto sulfide-selector intercalated Ni/Fe-LDH [23]. Another feasible mechanism was isomorphic substitution. Zhou and colleagues [24] found that the isomorphic substitution occurring between Pb^{2+}in solution and Mg^{2+} in the structure of Mn/Mg/Fe-LDH played an integral role in adsorption mechanism. Isomorphic substitution has been recognized by some other scholars for the adsorption of potentially toxic metals onto LDH-based materials [20].

In contrast, the adsorption process of $Cr_2O_7^{2-}$ and MnO_4^- anions onto LDH might involve anion exchange between the oxyanions in the solution and the anions (CO_3^{2-} and NO_3^-) in the interlayer region of LDH. A similar conclusion was reported by other scholars for adsorption of Cr(VI) onto Ni/Fe-LDH [10], polyaniline-modified Mg/Al-LDH [37], *in situ* synthesized Mg/Al-LDH [13], anisotropic Mg/Al-LDH nanosheets [14], and three-dimensional hierarchical flower-like Mg/Al-LDH [12]. Some detail information on the adsorption mechanism

Table 2: The corresponding parameters of the Langmuir and Freundlich models.

Unit		Cationic metals					Anionic metals	
		Cu^{2+}	Cd^{2+}	Ni^{2+}	Pb^{2+}	Cr^{3+}	$Cr_2O_7^{2-}$	MnO_4^-
(1) Langmuir model								
Q^o_{max}	mmol/g	0.601	0.880	1.299	0.657	0.701	0.589	0.522
K_L	L/mmol	0.493	0.742	1.630	1.546	1.072	1.282	0.602
Adj- R^2	—	0.985	0.988	0.991	0.986	0.982	0.985	0.994
χ^2	(×1000)	0.428	0.766	1.760	0.410	0.761	0.508	0.143
SD	—	0.023	0.030	0.045	0.021	0.030	0.025	0.013
MPSD	—	4.41	3.86	4.68	2.85	4.14	3.84	2.31
BIC	—	−51.4	−61.2	−47.7	−82.1	−61.3	−50.3	−76.3
(2) Freundlich model								
K_F	$(mmol/g)/(L/mmol)^n$	0.205	0.384	0.724	0.414	0.371	0.351	0.209
n	—	0.446	0.347	0.270	0.203	0.271	0.215	0.366
Adj- R^2	—	0.953	0.983	0.961	0.937	0.949	0.950	0.959
χ^2	(×1000)	1.390	1.120	7.730	0.477	2.220	1.740	0.882
SD	—	0.041	0.036	0.095	0.022	0.050	0.046	0.032
MPSD	—	5.26	4.14	8.09	3.17	6.29	5.16	3.94
BIC	—	−43.3	−57.8	−35.8	−81.5	−51.6	−41.7	−60.0

related to anionic exchange has been reported by Goh and coworkers [7]. Lastly, the mechanism of adsorption-coupled reduction has been identified during the process of Cr(VI) adsorption onto LDH-based materials. More detail information on such mechanism has been recently reviewed by Tran and colleagues [6].

4. Conclusions

The layered double hydroxide-based nanoadsorbent was successfully and rapidly synthesized from two low-cost metal salts of $Mg(NO_3)_2$ and $Al(NO_3)_3$ through the simple coprecipitation method. The basal spacing of LDH was 0.773 nm. LDH was nonporous material, with S_{BET} and V_{Total} being 23.2 m^2/g and 0.161 cm^3/g, respectively. The surface charge of LDH was positive within solution pH from 3.0 to 12. The CO_3^{2-} and NO_3^- anions existed abundantly in the interlayer region of LDH.

The Langmuir maximum adsorption capacity (Q^o_{max} ± standard deviation) of LDH towards various target toxic metals followed the decreasing order: Ni^{2+} (1.299 ± 0.029 mmol/g) > Cd^{2+} (0.880 ± 0.028 mmol/g) > Cr^{3+} (0.701 ± 0.023 mmol/g) > Pb^{2+} (0.657 ± 0.014mmol/g) > Cu^{2+} (0.601 ± 0.038 mmol/g) > $Cr_2O_7^{2-}$ (0.589 ± 0.038 mmol/g) > MnO_4^- (0.522 ± 0.015 mmol/g). It can be experimentally concluded that LDH was a promising dual-electronic adsorbent for effectively removing both toxic metal oxyanions and cations from the water environment. However, some further studies should be continued to feasibly apply this material for commercial purposes and real water treatment. They include the studies of adsorption column, regeneration, cost estimation, and toxicity.

Data Availability

No data were used to support this study.

Conflicts of Interest

The authors declare that they have no conflicts of interest.

Acknowledgments

This research is funded by Vietnam National Foundation for Science and Technology Development (NAFOSTED) under grant number 103.02-2019.54.

References

[1] F.-C. Huang, C.-K. Lee, Y.-L. Han, W.-C. Chao, and H.-P. Chao, "Preparation of activated carbon using micro-nano carbon spheres through chemical activation," *Journal of the Taiwan Institute of Chemical Engineers*, vol. 45, no. 5, pp. 2805–2812, 2014.

[2] S. Wong, N. Ngadi, I. M. Inuwa, and O. Hassan, "Recent advances in applications of activated carbon from biowaste for wastewater treatment: a short review," *Journal of Cleaner Production*, vol. 175, pp. 361–375, 2018.

[3] H. N. Tran, S.-J. You, and H.-P. Chao, "Fast and efficient adsorption of methylene green 5 on activated carbon prepared from new chemical activation method," *Journal of Environmental Management*, vol. 188, pp. 322–336, 2017.

[4] F. Tomul, Y. Arslan, B. Kabak et al., "Peanut shells-derived biochars prepared from different carbonization processes: comparison of characterization and mechanism of naproxen adsorption in water," *Science of The Total Environment*, vol. 726, article 137828, 2020.

[5] X. Liang, Y. Zang, Y. Xu et al., "Sorption of metal cations on layered double hydroxides," *Colloids and Surfaces A: Physicochemical and Engineering Aspects*, vol. 433, pp. 122–131, 2013.

[6] H. N. Tran, D. T. Nguyen, G. T. Le et al., "Adsorption mechanism of hexavalent chromium onto layered double hydroxides- based adsorbents: A systematic in-depth review," *Journal of Hazardous Materials*, vol. 373, pp. 258–270, 2019.

[7] K.-H. Goh, T.-T. Lim, and Z. Dong, "Application of layered double hydroxides for removal of oxyanions: a review," *Water Research*, vol. 42, no. 6-7, pp. 1343–1368, 2008.

[8] J. He, M. Wei, B. Li, Y. Kang, D. G. Evans, and X. Duan, "Preparation of layered double hydroxides," in *Layered Double Hydroxides*, X. Duan and D. G. Evans, Eds., pp. 89–119, Springer, 2006.

[9] S.-T. Lin, H. N. Tran, H.-P. Chao, and J.-F. Lee, "Layered double hydroxides intercalated with sulfur-containing organic solutes for efficient removal of cationic and oxyanionic metal ions," *Applied Clay Science*, vol. 162, pp. 443–453, 2018.

[10] G. Y. Abo El-Reesh, A. A. Farghali, M. Taha, and R. K. Mahmoud, "Novel synthesis of Ni/Fe layered double hydroxides using urea and glycerol and their enhanced adsorption behavior for Cr(VI) removal," *Scientific Reports*, vol. 10, no. 1, p. 587, 2020.

[11] M. Chakraborty, S. Dasgupta, C. Soundrapandian et al., "Methotrexate intercalated ZnAl-layered double hydroxide," *Journal of Solid State Chemistry*, vol. 184, no. 9, pp. 2439–2445, 2011.

[12] X.-Y. Yu, T. Luo, Y. Jia et al., "Three-dimensional hierarchical flower-like Mg–Al-layered double hydroxides: highly efficient adsorbents for As (V) and Cr(VI) removal,," *Nanoscale*, vol. 4, no. 11, pp. 3466–3474, 2012.

[13] H.-P. Chao, Y.-C. Wang, and H. N. Tran, "Removal of hexavalent chromium from groundwater by Mg/Al-layered double hydroxides using characteristics of in-situ synthesis," *Environmental Pollution*, vol. 243, pp. 620–629, 2018.

[14] H. Wang, S. Wang, Z. Chen, X. Zhou, J. Wang, and Z. Chen, "Engineered biochar with anisotropic layered double hydroxide nanosheets to simultaneously and efficiently capture Pb^{2+} and CrO_4^{2-} from electroplating wastewater," *Bioresource Technology*, vol. 306, article 123118, 2020.

[15] S.-H. Lee, M. Tanaka, Y. Takahashi, and K.-W. Kim, "Enhanced adsorption of arsenate and antimonate by calcined Mg/Al layered double hydroxide: investigation of comparative adsorption mechanism by surface characterization," *Chemosphere*, vol. 211, pp. 903–911, 2018.

[16] M. T. Rahman, T. Kameda, T. Miura, S. Kumagai, and T. Yoshioka, "Application of Mg–Al layered double hydroxide for treating acidic mine wastewater: a novel approach to sludge reduction," *Chemistry and Ecology*, vol. 35, no. 2, pp. 128–142, 2018.

[17] N. Ouasfi, M. Zbair, E. M. Sabbar, and L. Khamliche, "High performance of Zn–Al–CO_3 layered double hydroxide for anionic reactive blue 21 dye adsorption: kinetic, equilibrium, and thermodynamic studies," *Nanotechnology for Environmental Engineering*, vol. 4, no. 1, p. 16, 2019.

[18] Z. Zhu, S. Ouyang, P. Li, L. Shan, R. Ma, and P. Zhang, "Persistent organic pollutants removal via hierarchical flower-like layered double hydroxide: adsorption behaviors and mechanism investigation," *Applied Clay Science*, vol. 188, p. 105500, 2020.

[19] M. Shamsayei, Y. Yamini, and H. Asiabi, "Fabrication of zwitterionic histidine/layered double hydroxide hybrid nanosheets for highly efficient and fast removal of anionic dyes," *Journal of Colloid and Interface Science*, vol. 529, pp. 255–264, 2018.

[20] L.-X. Zhao, J.-L. Liang, N. Li, H. Xiao, L.-Z. Chen, and R.-S. Zhao, "Kinetic, thermodynamic and isotherm investigations of Cu^{2+} and Zn^{2+} adsorption on LiAl hydrotalcite-like compound," *Science of The Total Environment*, vol. 716, article 137120, 2020.

[21] A. T. Reda and D. Zhang, "Sorption of metal ions from aqueous solution by sulfonated calix[4]arene intercalated with layered double hydroxide," *Journal of Environmental Chemical Engineering*, vol. 7, no. 2, article 103021, 2019.

[22] M. T. Rahman, T. Kameda, S. Kumagai, and T. Yoshioka, "Effectiveness of Mg–Al-layered double hydroxide for heavy metal removal from mine wastewater and sludge volume reduction," *International journal of Environmental Science and Technology*, vol. 15, no. 2, pp. 263–272, 2018.

[23] J. Wang, L. Zhang, T. Zhang et al., "Selective removal of heavy metal ions in aqueous solutions by sulfide-selector intercalated layered double hydroxide adsorbent," *Journal of Materials Science & Technology*, vol. 35, no. 9, pp. 1809–1816, 2019.

[24] H. Zhou, Z. Jiang, and S. Wei, "A new hydrotalcite-like absorbent FeMnMg-LDH and its adsorption capacity for Pb^{2+} ions in water," *Applied Clay Science*, vol. 153, pp. 29–37, 2018.

[25] Y. Xu, Y. Ding, J. Wang et al., "In-situ synthesis of calcium aluminum layered double hydroxides for advanced treatment of leachate biochemical tail water," *Science of The Total Environment*, vol. 701, article 134891, 2020.

[26] H.-P. Chao and S.-H. Chen, "Adsorption characteristics of both cationic and oxyanionic metal ions on hexadecyltrimethylammonium bromide-modified NaY zeolite," *Chemical Engineering Journal*, vol. 193-194, pp. 283–289, 2012.

[27] H.-P. Chao, C.-K. Lee, L.-C. Juang, and Y.-L. Han, "Sorption of organic compounds, oxyanions, and heavy metal ions on surfactant modified titanate nanotubes," *Industrial & Engineering Chemistry Research*, vol. 52, no. 29, pp. 9843–9850, 2013.

[28] F. Chen, M. Hong, W. You, C. Li, and Y. Yu, "Simultaneous efficient adsorption of Pb^{2+} and MnO_4^- ions by MCM-41 functionalized with amine and nitrilotriacetic acid anhydride," *Applied Surface Science*, vol. 357, pp. 856–865, 2015.

[29] W. T. Reichle, "Catalytic reactions by thermally activated, synthetic, anionic clay minerals," *Journal of Catalysis*, vol. 94, no. 2, pp. 547–557, 1985.

[30] I. Langmuir, "The adsorption of gases on plane surfaces of glass, mica and platinum," *Journal of the American Chemical Society*, vol. 40, no. 9, pp. 1361–1403, 1918.

[31] H. Freundlich, "Über die Adsorption in Lösungen," *Zeitschrift für Physikalische Chemie*, vol. 57U, no. 1, pp. 385–470, 1907.

[32] H. N. Tran, S.-J. You, A. Hosseini-Bandegharaei, and H.-P. Chao, "Mistakes and inconsistencies regarding adsorption of contaminants from aqueous solutions: a critical review," *Water Research*, vol. 120, pp. 88–116, 2017.

[33] M. Kamari, S. Shafiee, F. Salimi, and C. Karami, "Comparison of modified boehmite nanoplatelets and nanowires for dye removal from aqueous solution," *Desalination and Water Treatment*, vol. 161, pp. 304–314, 2019.

[34] D. W. Marquardt, "An algorithm for least-squares estimation of nonlinear parameters," *Journal of the Society for Industrial and Applied Mathematics*, vol. 11, no. 2, pp. 431–441, 1963.

[35] G. Schwarz, "Estimating the dimension of a model," *The Annals of Statistics*, vol. 6, no. 2, pp. 461–464, 1978.

[36] C. Lei, X. Zhu, B. Zhu, C. Jiang, Y. Le, and J. Yu, "Superb adsorption capacity of hierarchical calcined Ni/Mg/Al layered double hydroxides for Congo red and Cr(VI) ions," *Journal of Hazardous Materials*, vol. 321, pp. 801–811, 2017.

[37] K. Zhu, Y. Gao, X. Tan, and C. Chen, "Polyaniline-modified Mg/Al layered double hydroxide composites and their application in efficient removal of Cr(VI)," *ACS Sustainable Chemistry & Engineering*, vol. 4, no. 8, pp. 4361–4369, 2016.

[38] M. Thommes, K. Kaneko, A. V. Neimark et al., "Physisorption of gases, with special reference to the evaluation of surface area and pore size distribution (IUPAC Technical Report)," *Pure and Applied Chemistry*, vol. 87, no. 9-10, pp. 1051–1069, 2015.

[39] F. R. Costa, A. Leuteritz, U. Wagenknecht, D. Jehnichen, L. Häußler, and G. Heinrich, "Intercalation of Mg–Al layered double hydroxide by anionic surfactants: preparation and characterization," *Applied Clay Science*, vol. 38, no. 3-4, pp. 153–164, 2008.

[40] W. Kagunya and W. Jones, "Aldol condensation of acetaldehyde using calcined layered double hydroxides," *Applied Clay Science*, vol. 10, no. 1-2, pp. 95–102, 1995.

[41] C. Moreno-Castilla, "Adsorption of organic molecules from aqueous solutions on carbon materials," *Carbon*, vol. 42, no. 1, pp. 83–94, 2004.

[42] S. Mechler, "Covid-19 pandemic: Face mask disinfection and sterilization for viruses," 2020, https://consteril.com/covid-19-pandemic-disinfection-and-sterilization-of-face-masks-for-viruses/.

[43] A. T. Vo, V. P. Nguyen, A. Ouakouak et al., "Efficient removal of Cr(VI) from water by biochar and activated carbon prepared through hydrothermal carbonization and pyrolysis: adsorption-coupled reduction mechanism," *Water*, vol. 11, no. 6, pp. 1164–1178, 2019.